

THERMODYNAMIC ANALYSIS OF MIXING OF Mn-Co BINARY ALLOY SYSTEM USING CALPHAD APPROACH

Mohib ullah khan¹, Dil faraz khan², Shahzeb burki³, Waseem ullah shah⁴, Haiqing yin⁵

¹Department of physics university of science & technology bannu, bannu 28100, kp pakistan.

² Department of physics university of science & technology bannu, bannu 28100, kp pakistan.

³ Department of physics university of science & technology bannu, bannu 28100, kp pakistan.

⁴ Department of physics university of science & technology bannu, bannu 28100, kp pakistan.

⁵School of meterial science and engineering, university of science and technology beijing, beijing 100083, pr china.

Abstract

This paper reports the variation of entropy and Gibbs energy of mixing of Mn and Co elements in Mn-Co binary alloy system using CALPHAD method. Entropy and Gibbs free energy of mixing were evaluated at four different elevated temperatures (i.e. 1125, 1225, 1325, and 1425K). It was observed that entropy decreases with the increase in temperature and maximum variation was observed in entropy at 40-43 atomic w% of Co as doping element in Mn base matrix. Corresponding negative deviations from Roults Law in Gibbs free energy curve indicated the stability of Mn-Co binary alloy system. Three types of phases were observed in this system having stable, unstable and metastable regimes. Variations in Gibbs energy were observed at the above mentioned temperatures.

Keyword: CALPHAD, Mn-Co Alloy, entropy, Gibbs energy curves, metastable phases.

1.INTRODUCTION

The Mn-Co alloy is very important and useful alloy due to its significant physical, mechanical and magnetic properties. The Mn-Co binary alloy system was first investigated by L. Kaufman in 1978[1].Analysing this main constituent of High Speed Steel (HSS) and High Entropy Alloys (HEAs), Mn-Co system gives strengthening through solid solution and enhances stability in microstructure for electroplating industry [2]. The Mn-Co system oxidizes at high temperature increases the conduction properties of large number of

cat ions formation [3]. Solid oxide fuel cells (SOFC) technologies case the system is oxidize to produce promising coating spinals found suitable candidates due to their high conductivity for SOFC interconnection applications [4]. The enhancements of large magnetic moments are due to a positive exchange interaction between Co and Mn in Mn-Co system is seen through neutron and XMCD (X-ray magnetic circular dichroism) formulism [5]. A.Z. Menshikov et al observed regions of ferromagnetic and antiferromagnetic order cascading magnetic phase diagram of Mn-Co system [6]. Weiming Haung in 1989 discussed the thermodynamic phase diagram and thermodynamic properties of Mn-Co binary alloy system [7].

2.TOOLS & TECHNIQUES

Computational thermodynamics were developed since 1970. We have used the Thermo-calc software with PBIN and FEDAT databases for simulation purposes in CALPHAD method. Thermo-calc is flexible and versatile software for simulation purposes of advance material alloys [8]. This software has large number of databases for pure metals and their alloys i.e. PBIN, PTERN, FEDAT etc. The CALPHAD technique (CALculation of PHase Diagram) is an old and important technique for evaluation of phase diagrams of alloy materials [9]. This technique is associated by thermodynamic modules such as Monte Carlo, ab initio, cluster variation method (CVM), density function theory (DFT) etc. [10].

3.THERMODYNAMIC MODULES

3.1.phase diagram

As the Mn-Co binary system was first discussed by L. Kaufmann and then by other researchers, gave data base of various thermodynamic properties [1]. Weiming Haung in 1989 gave an assessment of the system and showed six phases in phase diagram. He predicted about the seventh phase (sigma phase) after heavy deformation below 50 w% of Mn [7]. The phase diagram observed here shown accordance with Haung [7] by fig: 1 shows seven phases like CUB_A13, HCP_A3, FCC_A1#1, FCC_A1 #2, BCC_A2, CBCC_A12 and Liquid with no existence of sigma phase at 50%. At 0K three phases HCP_A3 at 0-40 at%, CUB_A13 at 50-70 at% and CBCC_A12 at 86-100 At% are present. The HCP_A3 phase at 693K totally transforms into FCC_A1#2 which make first appearance at 593K. At 413K, FCC_A1#1, the second largest and most stable phase of this system become active and maintain this stability and activity up to 1768K. The CBCC_A12 transforms totally into CUB_A13 at 783K. The CUB_A13 is the largest and second most stable phase; make transition in liquid region at 1433-1453K. The two temperatures 1433K and 1455K indicates two congruent points where CUB_A13 and BCC_A2 make transition to liquid phase. There is an another small phase, BCC_A2, lies at 1413-1519K with 90-100 at% of Co in Mn base matrix. The 1413K refers to a point known as Peritectoid where two solid phases (FCC_A1#1 and BCC_A2) mixed up to give a single solid phase (CUB_A13). Below 1768K all the phases are in solid phases and then make transition to Liquid phase. The FCC_A1#1 and HCP_A3 are with ferromagnetic domain while all other phases have anti ferromagnetic domains. These magnetic properties and oxidation states of Mn and Co elements make Mn-Co binary alloy system suitable candidate for SOFC (Solid Oxide Fuel Cell) and electroplating technologies.

Table1. Transition temperatures of various phases in phase diagram.

S/N o	Transitio n temp; in K (observe d)	Transitio n temp; in K (literatur e)	Phase transitions	
			1 st Phase	2 nd Phase
1	413	413.8	FCC_A1# 1	
2	593	586.46	FCC_A1# 2	
3	693	694.99	HCP_A3	FCC_A1# 2
4	783	980	CBCC_A1 2	CUB_A13
5	1363	1359.99	FCC_A1# 1	CUB_A13
6	1413	1419.92	FCC_A1# 1	BCC_A2
7	1433	1433.58	CUB_A13	Liquid
8	1453	1455.67	BCC_A2	Liquid
9	1519	1519	BCC_A2	Liquid
10	1768	1767.99	FCC_A1# 1	Liquid

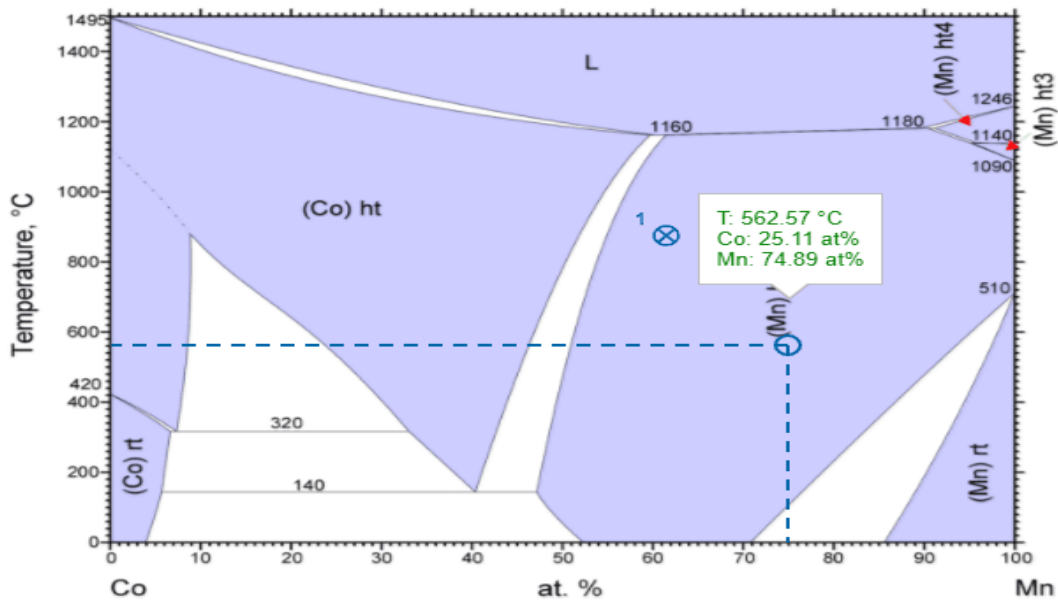


Figure1. Phase Diagram of Mn-Co binary alloy system showing various phases at transition temperatures.

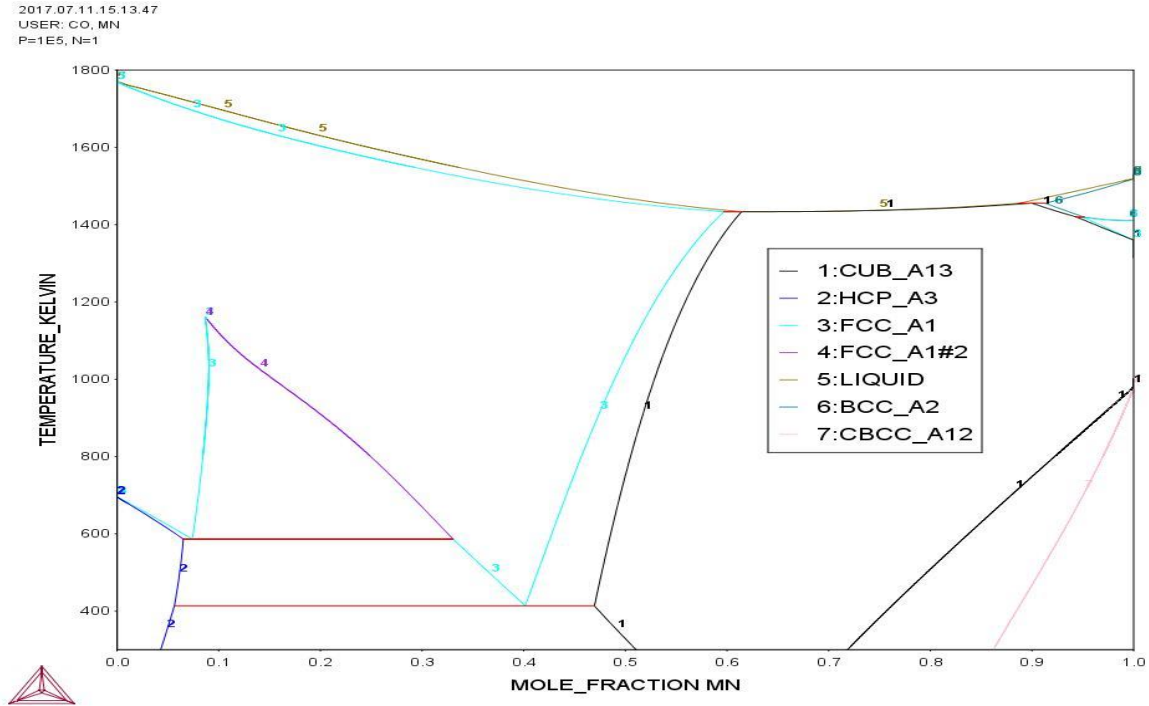


Figure2. Phase Diagram of Mn-Co binary alloy system including all the seven phases.

3.2. entropy

In Mn-Co binary alloy system, having Mn as base matrix and Co as an impurity (doping) element to the Mn matrix produces disorderness in Mn matrix shows the Co atoms defuses randomly in Mn base matrix [11-12].

Substitution solid solution is observed because of the closeness of sizes and atomic radii of both elements (127pm for Mn & 125pm for Co) [13]. Using Boltzmann's equation for evaluation of entropy of Mn-Co binary alloy system [14]

$$S = k_B \ln w \quad (1)$$

Where

$$w = \frac{N_{tot}!}{N_1!N_2!\dots N_n!} \quad (2)$$

and

$$N_{tot} = \sum_{i=1}^n N_i \quad (3)$$

N is the number of atoms of element *i* in *j* element system (*i*= Co & *j*=Mn)

From statistical mechanics, the Stirling's approximation for $\ln N$ with $N \gg 1$.

$$\Delta S_{mix} = -k_B \sum_{i=1}^j N_i \ln \frac{N_i}{N_{tot}} \quad (4)$$

For a system with partial ordering we can expand $n_{tot} = \sum_{k=1}^l n_k$ where n_{tot} is the sum of the number of moles *n* of sub lattice *k* for *l* number of sub lattices.

$$\Delta S_{mix} = -R \left[\sum_{k=1}^l n_k \sum_{i=1, i \neq m}^j x_{i,k} \ln x_{i,k} \right] \quad (5)$$

Where *m* is any element that is not included on that sub lattice.

Entropy change may be obtained in term of enthalpy of mixing as

$$dS = \left(\frac{dH}{T} \right)_P \quad (6)$$

$$dS = \left(\frac{dH}{T} \right)_P = \left(C_P \frac{dT}{T} \right) \quad (7)$$

$$\text{Thus } \Delta S = \int_{T_1}^{T_2} C_P \frac{dT}{T} = \int_{T_1}^{T_2} C_P d \ln T \quad (9)$$

ΔS can produces work and heat as a result. For a spontaneous mixing process $\Delta S > 0$, and for an equilibrium condition $\Delta S \leq 0$ [15].

THERMO-CALC (2017.10.13:12.53) :CO MN Temperature: 1125 K
DATABASE:PBIN

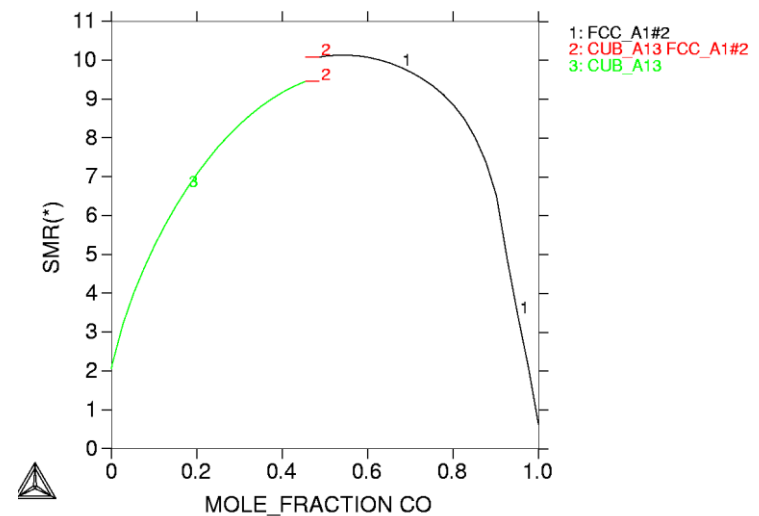


Figure3 (a)

THERMO-CALC (2017.10.13:12.55) :CO MN Temperature: 1225 K
DATABASE:PBIN

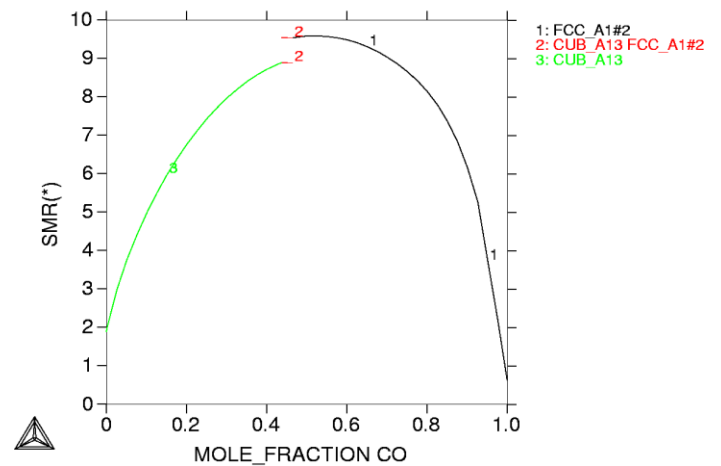


Figure3(b)

THERMO-CALC (2017.10.13:13.04) :CO MN Temperature: 1325 K
 DATABASE:PBIN

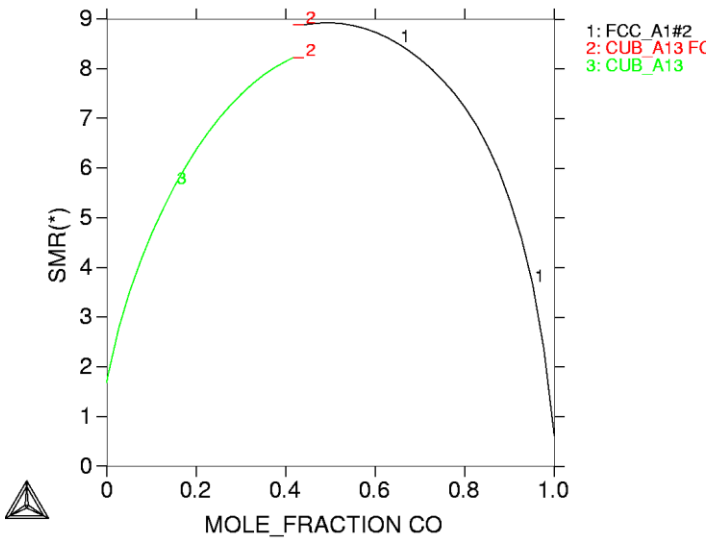


Figure3(c)

THERMO-CALC (2017.10.13:13.05) :CO MN Temperature: 1425 K
 DATABASE:PBIN

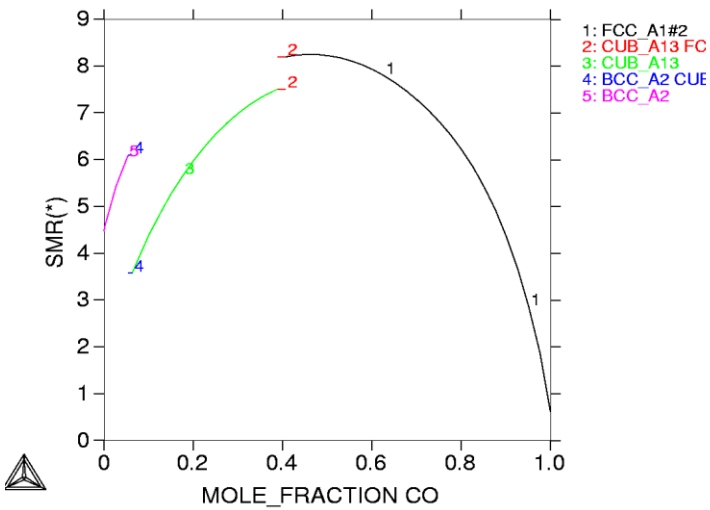


Figure3 (d)

Figure3: entropy curves of major phases at different temperatures (a) at 1125K, (b) at 1225K, (c) 1325K and (d) at 1425K.

THERMO-CALC (2017.10.05:14.54) :CO MN Mole-fraction CO : .2
 DATABASE:PBIN
 N=1., P=100000,X(CO)=3E-1;

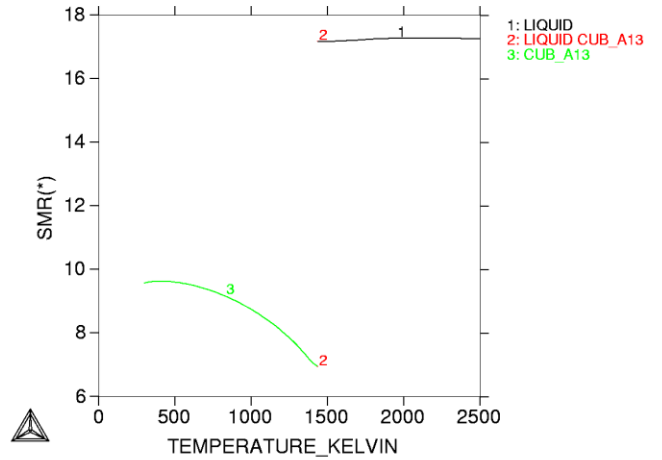


Figure4 (a)

THERMO-CALC (2017.10.05:14.52) :CO MN Mole-fraction CO : .3
 DATABASE:PBIN
 N=1., P=100000,X(CO)=3E-1;

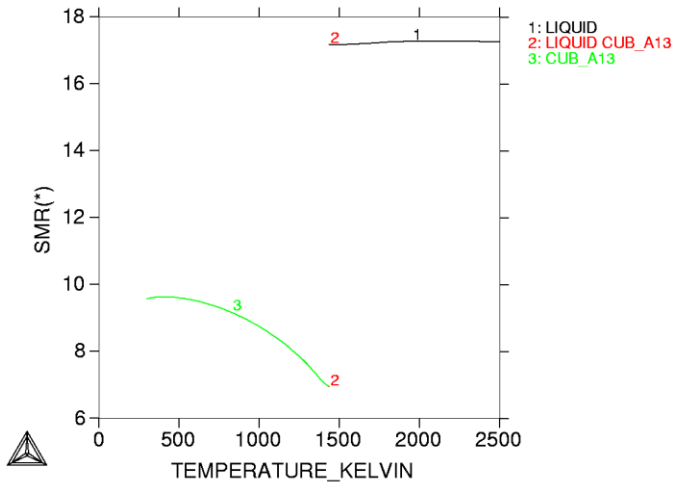


Figure4 (b)

Fig:4 (a,b), showing variation of Entropy of Mixing at two different mole fractions of Co (0.2 and 0.3) plotted against temperature upto 2500K.

Entropy vs. Mole Fraction at N=1, P=100000

S/N o	Active phases	X(Co) % Range	Max Entropy (J/mol.K) at Temp; (K)			
			1125	1225	1325	1425
1	CUB_A13	0-42	9.2	8.9	8.2	7.5
2	FCC_A1# 2	45-100	10	9.6	8.9	8.2
3	BCC_A2	0-10	---	---	---	6.1
4	Miscibility Gap 1	42-45	---	---	---	---
5	Miscibility Gap 2	5-7	---	---	---	---

Table 2. showing maximum entropy at four different elevated temperature (1125,1225,1325 and 1425K).

Entropy vs. Temperature at N=1, P=100000

S/N o	Active Phases	Temp; Range(K)	Max Entropy(J/mol.K)/temp;(K)	X(Co) %
1	CUB_A13	300-1400	9.5/300	20-30
2	Liquid	1410-.....	17/1500	20-30
3	Miscibility Gap	1400-1410	---	20-30

Table 3. showing maximum entropy at particular temperature at mole fraction of Co 0.2-0.3 or 20-30%.

3.3. gibbs free energy of mixing

A small change in any of system parameter p, v and T can cause an infinitesimal change in Gibbs energy of the system.

$$\Delta G = \Delta U - T\Delta S + P\Delta V \quad (10)$$

$$\Delta G_{mix} = \Delta H_{mix} - T\Delta S_{mix} \quad (11)$$

H is enthalpy of mixing, when $\Delta S < 0, \Delta H > 0$ and $\Delta G > 0$ (positive). The process of mixing will be non-spontaneous and endothermic. But when $\Delta S > 0, \Delta H < 0$ and $\Delta G < 0$ (negative), the process of mixing will be spontaneous and exothermic [16]. from fig 5, the Gibbs energy of our system is negative; the process of mixing is spontaneous.

Before mixing the total Gibbs energy is the sum of the Gibbs energies of Mn and Co, the constituent elements [17].

$$G_{Mn} + G_{Co} = n_{Mn}\mu_{Mn}^{pure}(T, P) + n_{Co}\mu_{Co}^{pure} \quad (12)$$

where μ is chemical potential of Mn and Co elements in pure form.

After mixing the total Gibbs energy of the mixture is the sum of Gibbs energies of Mn and Co in the mixture [18].

$$G_{mix} = n_{Mn}\mu_{Mn}(T, P, n_{Mn}, n_{Co}) + n_{Co}\mu_{Co}(T, P, n_{Mn}, n_{Co}) \quad (13)$$

$$G_{mix} = n_{Mn}[\mu_{Mn}^{pure}(T, P) + RT \ln X_{Mn}] + n_{Co}[\mu_{Co}^{pure}(T, P) + RT \ln X_{Co}] \quad (14)$$

$$G_{mix} = n_{Mn}\mu_{Mn}^{pure}(T, P) + n_{Co}\mu_{Co}^{pure}(T, P) + n_{Mn}RT \ln X_{Mn} + n_{Co}RT \ln X_{Co} \quad (15)$$

Subtracting equation: 13 from equation: 15, we get;

$$\Delta G_{mix} = n_{Mn}RT \ln X_{Mn} + n_{Co}RT \ln X_{Co} \quad (16)$$

$$\Delta G_{mix} = nRT(X_{Mn} \ln X_{Mn} + X_{Co} \ln X_{Co}) \quad (17)$$

Where

$$n = n_{Mn} + n_{Co}$$

and

$$X_{Co} = 1 - X_{Mn}$$

Gibbs energy is always negative for spontaneous and exothermic mixing. The Gibbs energy is zero whenever X_{Mn} or $X_{Co} = 1$ and is minimum whenever $X_{Mn} = X_{Co}$. It is clear from equation (17) that Gibbs energy of mixing is related to entropy of mixing [19].

Figure5 (a)

THERMO-CALC (2017.10.05:14.27) :CO MN Temperature: 1125 K
 DATABASE:PBIN
 P=100000, N=1, T=1125;

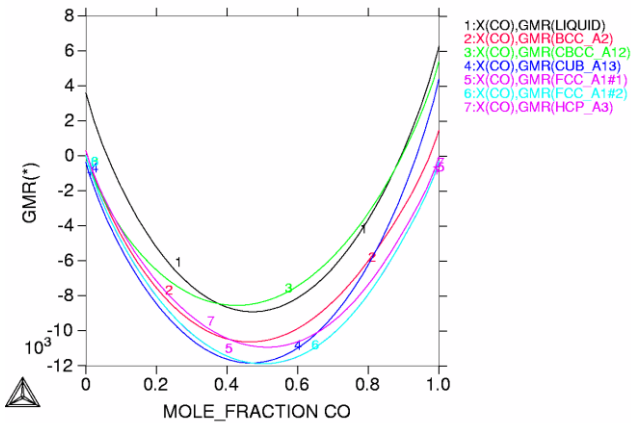


Figure5 (c)

THERMO-CALC (2017.10.05:14.29) :CO MN Temperature: 1325 K
 DATABASE:PBIN
 P=100000, N=1, T=1325;

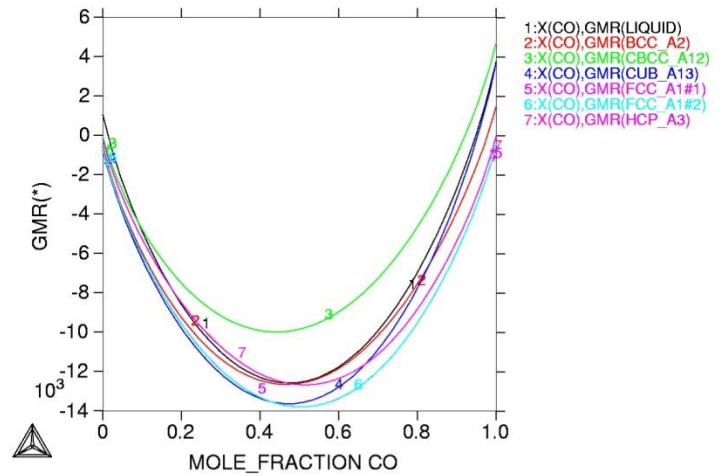


Figure5 (d)

THERMO-CALC (2017.10.05:14.30) :CO MN Temperature: 1425 K
 DATABASE:PBIN
 P=100000, N=1, T=1425;

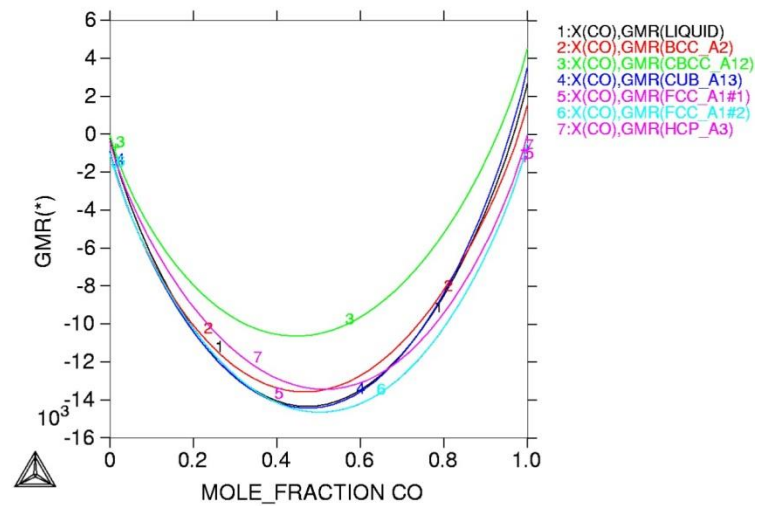


Figure5

THERMO-CALC (2017.10.05:14.28) :CO MN Temperature: 1225 K
 DATABASE:PBIN
 P=100000, N=1, T=1225;

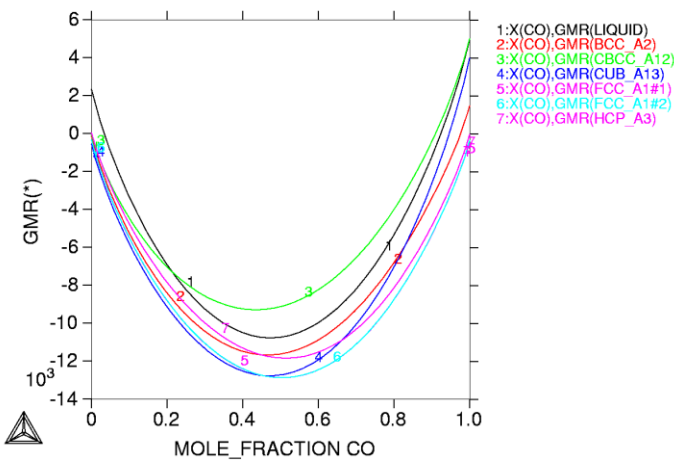


Figure 5: showing variation in Gibbs energy curve at (a) 1125K, (b) 1225K, (c) 1325K and (d) 1425K.

Table5: Thermodynamic phase equilibria calculation of Mn-Co binary alloy system at P=10⁵

S/No	Temp K	Active Phase	Components	Moles	W/ fraction	Activity	Chemical Potential	Ref stat
1	1125	FCC_A1#1	Mn	9.9814E-01	9.9800E-01	2.4050E+03	-5.6405E+04	SER
			Co	1.8647E-03	2.0000E-03	7.4984E-07	-1.3192E+04	SER
2	1225	FCC_A1#1	Mn	9.9814E-01	9.9800E-01	1.7922E-03	-6.4415E+04	SER
			Co	1.8647E-03	2.0000E-03	6.6967E-07	-1.4480E+05	SER
3	1325	FCC_A1#1	Mn	9.9814E-01	9.9800E-01	1.3562E-03	-7.2744E+04	SER
			Co	1.8647E-03	2.0000E-03	5.9337E-07	-1.5795E+05	SER
4	1425	BCC_A2#1	Mn	9.9814E-01	9.9800E-01	1.0384E-03	-8.1398E+04	SER
			Co	1.8647E-03	2.0000E-03	5.2001E-07	-1.7144E+05	SER

Table6: Thermodynamic Gibbs energy and entropy calculation of Mn-Co binary alloy system.

S/No	Temp:	Active phase	No of Moles	Mass	Volume	Gibbs energy	Enthalpy
1	1125K	FCC_A1#1	1.00000	5.49454E+04	0.00000E+00	-5.65462E+04	3.17978E+04
2	1225K	FCC_A1#1	1.00000	5.49454E+04	0.00000E+00	-6.45647E+04	3.56556E+04
3	1325K	FCC_A1#1	1.00000	5.49454E+04	0.00000E+00	-7.29032E+04	3.96324E+04
4	1425K	BCC_A2#1	1.00000	5.49454E+04	0.00000E+00	-8.15658E+04	4.56800E+04

4.RESULTS &DISCUSSIONS

Entropy curve at four elevated temperatures (1125, 1225, 1325, and 1425K) was investigated. Two stable phases with varying entropies were observed in composition range 0-100 w% at temperature 1125 K. The CUB_A13 phase was found with positive entropy up to 9%, the maximum in entropy was observed at 40-45 atomic weight per cent of Co. The FCC_A1#2 phase was seen a phase with negative entropy, the entropy decreased with increase in molar concentration of Co element in Mn base matrix resulting in cluster formation. The CUB_A13 phase lies in molar concentration range 0-43 atomic w% of Co having entropy 2-9.5%. The FCC_A1#2 phases appears at 42-100% of Co with a decrease in entropy from 10 to 2% as shown in fig; 3(a,b,c,d).

At 1225K the entropy values drops from 10 to 0.9% for FCC_A1#2 and 8.9% for CUB_A13, FCC_A1#2 with 8% for CUB_A13 phase at 1325K. At 1425K phase with positive entropy range found (BCC_A2 < CUB_A13) which is having entropy range 4.5-6.1% in 0-1atm w% of Co in Mn base matrix.

It is observed that the entropy of solid phases decreases with increase in temperature at constant amount of doping material in prescribed alloy system.

The Gibbs energy becomes more negative with increase in temperature. The negative value of Gibbs energy indicates the stability of the system and is a consequence of deviation from Roults Law shows spontaneous and exothermic mixing [20]. This system is also in accordance with regular solution model and great incorporation of high entropy and negative Gibbs energy of mixing [21]. The more stable phases present in Mn-Co binary system are FCC_A1#2 and CUB_A13 with highest negative Gibbs energy and high entropy and can be utilized in well industrial needs. There is also a least stable phase CBCC_A12. The metastable phases that appear in this system are BCC_A12, FCC_A1#1 and HCP_A3 as clear from fig: 5 (a, b,c,d).

5.INDUCED MISCIBILITY GAP

A miscibility gap was found in range 40-45atm w% of Co in Mn base matrix and temperature range approaching to 1500K as shown in fig:3. At temperatures 1125-1325K the only miscibility gap is between FCC_A1#2 and CUB_A13 phases, at temperature 1425K, fluctuation gap as

predicted one between FCC_A1#and CUB_A13 and the second one between CUB_A13 and BCC_A2 phases. The induced miscibility gap is major characteristic of transition metal alloys with fluctuating nature of phases present within.

6.CONCLUSIONS

1. In course there occurs a decrease in entropy with increase in temperature. The entropy of the system is maximum below 500K for all solid phases.
2. Approximately constant behaviour in entropy above 1500k at 16-18% w CBCC_A12 were observed with system in liquid state as unstable. Entropy of the system near to 1500K minimum for all solid phases and maximum for liquid phase.
3. The reduction in entropy after reaching maximum is due to Cluster formation (clotting of Co atoms)
4. CUB_A13 is the phase of positive entropy up to 9-10%. The phase of negative entropy is FCC_A1#2, with maximum entropy of 10% at 40-50atm w% of Co.
5. A gap occurs between two phases in entropies near 1500K and 40-43atm w% of Co. At temp; 1425K phase BCC_A2 with entropy 4.5-6% for 0-1atm w% of Co. unstable and metastable phases co-exist in our prescribed alloy system.
6. The stable phases observed with highest negative value of Gibbs energy are FCC_A1#2 , CUB_A13 in the range 40-50 w% of Co. clotting of Co atoms is observed at above Particular concentrations in alloy. The stability and perfect order of entropies of the above mention phases will make the prescribed system industrially and commercially important.

7.ACKNOWLEDGEMENT

I am really very thankful to all mighty Allah for giving me such a wonderful opportunity and guidance and removing all the difficulties throughout all the research work.

I am also glade to thanks my parents and family members for supporting me throughout all the research work. I am also well-wisher and thankful to Dr. Dilfaraz

Khan (Chairman Dept.: of Physics UST Bannu KP Pakistan) and Haiqing Yin (UST Beijing , PR China) to providing us such a beneficial software, Thermo-calc. This work is not supported by any govt: and other organisational financial aid.

REFERENCES

- [1] Larry Kaufman (1978) Coupled Phase Diagrams and Thermochemical Data for Transition Metals Binary systems-III, CALPHAD vol.2, No.2, pp. 117-146.
- [2] J. Wu *et al* (2008) DC Electro deposition of Mn-Co alloys on stainless steel for SOFC interconnect application, Journal of Power Sources, 177, pp.376-385.
- [3] M.E. El-Dahshan (1982) The Oxidation of Cobalt-Manganese alloys at High Temperature, Transaction of the Japan Institute of Metals, vol.23, No.4, pp.177-185.
- [4] J. Wu *et al* (2008), Pulse Plating of Mn-Co alloys for SOFC interconnect applications, Electrochimica Acta, 54, pp.793-800.
- [5] T.H. Kim *et al* (2002), Enhanced Ferromagnetism and Spin-polarized tunnelling Studies on Co-Mn alloy films, PHYSICAL REVIEW B, 66,104436.
- [6] A.Z. Menshikov *et al*, The Magnetic Phase Diagram of Mn-Co alloys, Zh. Eksp. Teor. Fiz. 89.
- [7] W. Haung *et al* (1989), An Assessment of Co-Mn system, CALPHAD vol.13,-No.3, pp.231-242.
- [8] J.O. Anderson *et al* (2002), THERMO-CALC & DICTRA, Computational Tools For Materials Science, Calphad vol.32, No.2, pp.273-312.
- [9] C.E. Campbell *et al* (2014), The Development of Phase Based Property data using the CALPHAD method and infrastructure needs, Integrated Materials and Manufacturing Innovation, pp.3-12.
- [10] R. Otis *et al* (2017), SOFTWARE METAPAPER pycalphad: CALPHAD-based Computational Thermodynamics in Python, Journal of Open Research Software, 5:1.
- [11] F. Otto *et al* (2013), Relative effects on enthalpy and entropy on the phase stability of equiatomic High Entropy Alloys, Acta Materialia, xx, xxx.
- [12] L.J. Cuddy *et al* (1972), Some Aspect of Serrated Yielding in Substitutional Solid Solutions of Iron, ACTA METALLURGICA, vol.20, 1157.
- [13] Z.L. Sheng *et al* (2013), Recent Progress in High-entropy Alloys, Advance Materials Research, vol.631-32, pp. 227-232.
- [14] J.F. Chinella *et al* (2011), Computational Thermodynamics Characterization of 7075, 7039, and 7020 Aluminium Alloys Using JMatPro, Army Research Laboratory, ARL-TR-5660.
- [15] E-AN. Zen *et al* (1972) Gibbs free energy, enthalpy and entropy of ten rock forming minerals: calculation, discrepancies, implications, , American mineralogist, vol.57, pp.524-553.
- [16] K. C. Harry Kumar *et al* (1994), Thermodynamic calculation of Nb-Ti-V phase diagram, Calphad vol: 18, pp71-79.
- [17] SchloB Ringberg (1997), Thermodynamic modelling of solution and alloy, Calphad vol: 21, pp. 171-218.
- [18] W. Huang (1989), An Assessment of the Co-Mn System CALPHAD Vol. 13, No. 3, pp. 231-242.
- [19] Campbell *et al* (2014) The development of phase based property data using Calphad method and infrastructure needs, Integrating Materials and Manufacturing Innovation 2014, 3:12.
- [20] John F. Chinella and Zhanli Guo (2011), Computational Thermodynamics 75, 7039, and 7020 Aluminium Alloys Using JMatPro, Army Research Laboratory Aberdeen Proving Ground.
- [21] T. Nishizawa *et al* (, 1979), Thermodynamic analysis of solubility and miscibility gap in Ferromagnetic Alpha Iron Alloy, Acta Metallurgica, vol.27, pp.817-828.